

Polarization-independent active metamaterial for high-frequency terahertz modulation

Oliver Paul¹, Christian Imhof², Bert Lagel³, Sandra Wolff³, Jan Heinrich⁴, Sven Hoffling⁴, Alfred Forchel⁴, Remigius Zengerle², Rene Beigang^{1,5}, and Marco Rahm^{1,5}

¹*Department of Physics, University of Kaiserslautern, Germany*

²*Department of Electrical and Computer Engineering, University of Kaiserslautern, Germany*

³*Center for Nanostructure Technology and Biomolecular Technology, University of Kaiserslautern, Germany*

⁴*Department of Applied Physics, University of Wurzburg, Germany*

⁵*Fraunhofer Institute for Physical Measurement Techniques IPM, Freiburg, Germany*

paul@physik.uni-kl.de

Abstract: We present a polarization-independent metamaterial design for the construction of electrically tunable terahertz (THz) devices. The implemented structure consists of an array of gold crosses fabricated on top of an n-doped gallium arsenide (GaAs) layer. Utilizing THz time-domain spectroscopy, we show that the electric resonance and thus the transmission properties of the cross structure can be tuned by an externally applied bias voltage. We further demonstrate the fast amplitude modulation of a propagating THz wave for modulation frequencies up to 100 kHz.

© 2008 Optical Society of America

OCIS codes: (160.3918) Metamaterials; (230.4110) Modulators; (300.6495) THz spectroscopy; (220.4000) Microstructure

References

1. J. B. Pendry, "Negative Refraction Makes a Perfect Lens," *Phys. Rev. Lett.* **85**, 3966–3969 (2000).
2. V. D. Veselago, "The electrodynamics of substances with simultaneously negative values of ϵ and μ ," *Soviet Physics Uspekhi* **10**, 509–514 (1968).
3. D. R. Smith, W. J. Padilla, D. C. Vier, S. C. Nemat-Nasser, and S. Schultz, "Composite Medium with Simultaneously Negative Permeability and Permittivity," *Phys. Rev. Lett.* **84**, 4184–4187 (2000).
4. V. M. Shalaev, W. Cai, U. K. Chettiar, H.-K. Yuan, A. K. Sarychev, V. P. Drachev, and A. V. Kildishev, "Negative index of refraction in optical metamaterials," *Opt. Lett.* **30**, 3356–3358 (2005).
5. S. Zhang, W. Fan, N. C. Panoiu, K. J. Malloy, R. M. Osgood, and S. R. J. Brueck, "Experimental Demonstration of Near-Infrared Negative-Index Metamaterials," *Phys. Rev. Lett.* **95**, 137404 (2005).
6. C. Imhof and R. Zengerle, "Pairs of metallic crosses as a left-handed metamaterial with improved polarization properties," *Opt. Express* **14**, 8257–8262 (2006).
7. M. Gokkavas, K. Guven, I. Bulu, K. Aydin, R. S. Penciu, M. Kafesaki, C. M. Soukoulis, and E. Ozbay, "Experimental demonstration of a left-handed metamaterial operating at 100 GHz," *Phys. Rev. B* **73**, 193103 (2006).
8. O. Paul, C. Imhof, B. Reinhard, R. Zengerle, and R. Beigang, "Negative index bulk metamaterial at terahertz frequencies," *Opt. Express* **16**, 6736–6744 (2008).
9. C. Imhof and R. Zengerle, "Strong birefringence in left-handed metallic metamaterials," *Opt. Commun.* **280**, 213–216 (2007).
10. E. Plum, V. A. Fedotov, A. S. Schwanecke, N. I. Zheludev, and Y. Chen, "Giant optical gyrotropy due to electromagnetic coupling," *Appl. Phys. Lett.* **90**, 223113 (2007).

11. W. J. Padilla, A. J. Taylor, C. Highstrete, M. Lee, and R. D. Averitt, "Dynamical Electric and Magnetic Metamaterial Response at Terahertz Frequencies," *Phys. Rev. Lett.* **96**, 107401 (2006).
12. H.-T. Chen, J. F. O'Hara, A. K. Azad, A. J. Taylor, R. D. Averitt, D. B. Shrekenhamer, and W. J. Padilla, "Experimental demonstration of frequency-agile terahertz metamaterials," *Nat. Photonics* **2**, 295–298 (2008).
13. J. Han, A. Lakhtakia, and C.-W. Qiu, "Terahertz metamaterials with semiconductor split-ring resonators for magnetostatic tunability," *Opt. Express* **16**, 14390–14396 (2008).
14. H.-T. Chen, W. J. Padilla, J. M. O. Zide, A. C. Gossard, A. J. Taylor, and R. D. Averitt, "Active terahertz metamaterial devices," *Nature* **444**, 597–600 (2006).
15. H.-T. Chen, H. Lu, A. K. Azad, R. D. Averitt, A. C. Gossard, S. A. Trugman, J. F. O'Hara, and A. J. Taylor, "Electronic control of extraordinary terahertz transmission through subwavelength metal hole arrays," *Opt. Express* **16**, 7641–7648 (2008).
16. H.-T. Chen, S. Palit, T. Tyler, C. M. Bingham, J. M. O. Zide, J. F. O'Hara, D. R. Smith, A. C. Gossard, R. D. Averitt, W. J. Padilla, N. M. Jokerst, and A. J. Taylor, "Hybrid metamaterials enable fast electrical modulation of freely propagating terahertz waves," *Appl. Phys. Lett.* **93**, 091117 (2008).
17. A. N. Lagarkov and A. K. Sarychev, "Electromagnetic properties of composites containing elongated conducting inclusions," *Phys. Rev. B* **53**, 6318–6336 (1996).
18. J. B. Pendry, A. J. Holden, W. J. Stewart, and I. Youngs, "Extremely Low Frequency Plasmons in Metallic Mesostructures," *Phys. Rev. Lett.* **76**, 4773–4776 (1996).
19. A. Mackay, "Proof of polarisation independence and nonexistence of crosspolar terms for targets presenting n -fold ($n > 2$) rotational symmetry with special reference to frequency-selective surfaces," *Electron. Lett.* **25**, 1624–1625 (1989).
20. T. Kleine-Ostmann, P. Dawson, K. Pierz, G. Hein, and M. Koch, "Room-temperature operation of an electrically driven terahertz modulator," *Appl. Phys. Lett.* **84**, 3555–3557 (2004).

1. Introduction

During the last years, metamaterials have gained a lot of scientific interest. The main benefit of such artificially structured materials is the possibility to tailor their electromagnetic properties even beyond the boundaries of naturally occurring materials. This offers a large number of new opportunities for the design of electromagnetic and optical devices. Following these new concepts, a lot of interesting applications for metamaterials have been proposed. One of the most prominent examples propelling the research field of metamaterials is the perfect lens [1], capable of focusing electromagnetic waves beyond the diffraction limit. This device is based on the physical phenomenon of negative refraction [2–8]. Other interesting applications aim at the manipulation of the polarization state of electromagnetic radiation. By using artificial metastructures it was possible to design materials with strong polarization rotatory power [9, 10] being up to five orders of magnitude higher than in any chiral material occurring in nature. In the context of the so called terahertz gap (0.1 – 10 THz) where nearly no naturally occurring material exists for the efficient construction of functional elements, metamaterials are a promising candidate to fill up this gap and enable a more efficient access to the various applications of terahertz waves.

Recently, active metamaterials have been proposed which allow the control of the transmission and reflection properties of metamaterials by illuminating the structure with laser light [11, 12], by varying an external magnetostatic field [13] or by using an external bias voltage supply [14–16]. These methods pave the way to a wide field of applications from high-sensitive spectroscopy to short-range secure THz communication. However, all structures presented so far have been designed in a way that the desired electromagnetic response of the metamaterial is only supported for a pre-defined linear polarization state of the incident light. On the other hand, for many applications like reflection spectroscopy, ellipsometry or even the investigation of atomic states or the electromagnetic response of polar media, it is necessary to work with elliptically polarized waves, waves with changing direction of the linear polarization or even unpolarized light. Furthermore, some optical components, especially fibers, change the polarization state of transmitted light in an unpredictable manner and often the source of the radiation itself is an emitter of unpolarized waves. For all these cases, the implementation of

active metamaterials requires polarization-insensitive design concepts.

In this paper we report the design, fabrication and characterization of an electrically tunable metamaterial-based modulator for THz radiation. The metamaterial is composed of symmetric unit cell structures to ensure polarization-insensitive behavior with respect to incident waves of arbitrary polarization.

2. Structure design and fabrication

A schematic layout of the implemented structure including all geometrical parameters is shown in Fig. 1. The metamaterial is composed of an array of gold crosses fabricated on top of an n-doped GaAs layer. The cross bars are 80 μm long, 10 μm wide and are separated by a 1 μm wide gap. Additionally, all crosses are electrically interconnected by 1 μm thin wires whose effect on the electric resonance of the cross structure can be neglected. The n-doped GaAs layer was grown on a semi-insulating GaAs substrate by molecular beam epitaxy. To improve the electric transition within the GaAs we used a doping profile consisting of a 1500 nm thick Si-doped GaAs layer ($n = 5 \cdot 10^{16} \text{ cm}^{-3}$), a 250 nm thick linearly graded Si-doped GaAs layer ($n = 5 \cdot 10^{16} \text{ cm}^{-3}$ to $n = 5 \cdot 10^{18} \text{ cm}^{-3}$) followed by a 100 nm thick highly Si-doped GaAs top layer ($n = 5 \cdot 10^{18} \text{ cm}^{-3}$). In the next step, the ohmic contact strip was produced by electron beam evaporation of 20 nm nickel, 20 nm germanium and 150 nm gold, followed by a rapid thermal annealing process at 350 $^{\circ}\text{C}$ for 1 min in nitrogen atmosphere. Thereafter, the cross structure was patterned by standard electron beam lithography and metallized by deposition of 150 nm gold on a 10 nm titanium adhesion layer. This leads to the formation of a Schottky contact between the cross structure and the n-doped GaAs top layer. We finally applied bond wires to the contact pads of the structure to connect the device with an electrical circuit.

The electromagnetic properties of the cross structure, which is basically a two-dimensional version of a cut wire, can be easily derived from [4, 17]. The crossbars act as small electrical dipoles which can be excited by an incident electromagnetic field, thus leading to a negative effective permittivity in the vicinity of the resonance frequency of the structure. Since the ma-

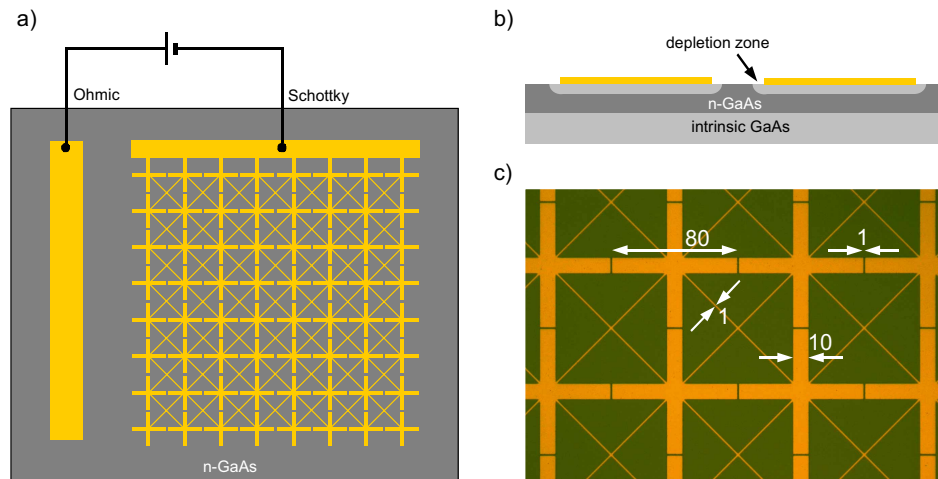


Fig. 1. a) Schematic layout of the implemented cross structure with externally tunable bias supply. b) Lateral cut of the structure on semi-insulating GaAs with illustrated depletion zone under reverse bias. c) Microscope picture of the fabricated structure with indicated dimensions in μm .

major fraction of the electromagnetic wave is reflected from the metamaterial surface for negative values of the permittivity (permeability is positive), the associated transmission spectrum through the metamaterial layer exhibits a stop band around the dipole resonance frequency.

However, the transmission characteristics of the metamaterial can be purposely tuned by controlling the conductivity of the n-doped GaAs layer. In the case where the conductivity is sufficiently high, the crosses are effectively shortened along the small gap between their ends and the metamaterial is transformed into a continuous wire structure [18]. Since the corresponding plasma frequency is well below the THz frequency range, THz waves can be transmitted through the medium with moderate loss. At this point, it should be mentioned that the presented metamaterial structure has not been optimized for impedance matching with free space so that the transmitted wave inherently suffers from insertion loss at the input facet of the metamaterial layer. In contrast, if a reverse bias is applied to the electrodes, a depletion region for free carriers is formed around the crosses (see Fig. 1(b)) and the horizontal and vertical bars are no longer shortened. This leads to the formation of separated dipoles whose resonance frequency is located in the THz frequency range. Consequently, the metamaterial appears to be virtually opaque for THz waves. The dependence of the substrate conductivity in the depletion region on the reverse bias voltage can thus be used to control the transmission characteristics of the device. Since the implemented cross structure is invariant under rotation of 90° , the arising transmission properties are independent of the polarization of the propagating THz wave [6, 19].

3. Results and discussion

3.1. Electric circuit characterization

To analyze the electrical properties of the metamaterial device we determined the current-voltage characteristics of the structure by varying the applied external voltage between -15 V and 2 V and measured the current driven through the metamaterial. As expected, the results shown in Fig. 2(a) reveal a typical Schottky diode characteristic. As can be seen, the reverse saturation current above -14 V is smaller than 1 mA. This means that the formation of a charge depletion region between the crosses with appropriate insulation efficiency is adequately supported by the electric circuit at a reverse bias voltage above -14 V.

Since the modulation speed of the metamaterial-based THz modulator is strongly related to a quick formation of the charge depletion zone between the crosses, we analyzed the current response to an applied voltage pulse. For this purpose we used a signal frequency synthesizer

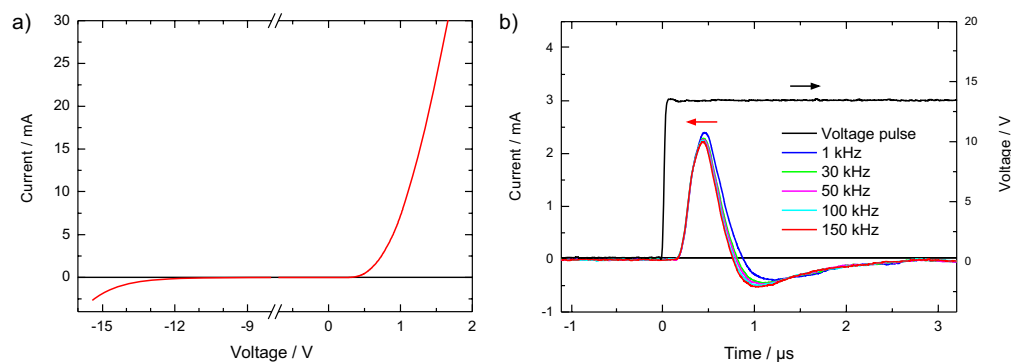


Fig. 2. a) Current-voltage characteristic of the implemented structure. b) Time-sensitive current response to a rectangular voltage pulse.

to square wave modulate the reverse bias voltage between -13.3 V and 0 V at frequencies up to 150 kHz. The current response of the structure was amplified by a low noise current amplifier (*Femto DLPCA-200*) with a gain of 10^3 V/A and analyzed on a digital oscilloscope. The results presented in Fig. 2(b) show a damped resonant behavior of the current which is caused by the capacitance of the depletion region, the Schottky forward resistance and the inductance of the leads. The measurements show that the charge equalization is completed within $t_c = 2.7 \mu\text{s}$, independent of the applied modulation frequency. The fraction of the half cycle duration T_H of the applied modulation signal, where the depletion zone is completely formed, is given by

$$F = \frac{T_H - t_c}{T_H} = 1 - 2t_c f$$

where $f = 1/(2T_H)$ is the modulation frequency. Consequently, the modulation ability of the device will decrease for increasing frequencies and finally break down. If we suppose that the modulation magnitude of a propagating THz wave is proportional to F , the 50% cutoff frequency of the device can be approximated to be

$$f_{cut} \approx \frac{1}{4t_c} = 93 \text{ kHz}$$

3.2. THz transmission properties

The transmission properties of the proposed device are analyzed by a THz time-domain system which is depicted in Fig. 3. It basically consists of a femtosecond laser, the THz section with the metamaterial sample in focus, a delay line to vary the timing of the detection pulse and the electronic measuring equipment. The system operates with linearly polarized THz waves which are focused normally to the metamaterial surface to a spot size of 1.5 mm.

We first analyzed the transmission through the metamaterial for different values of an applied DC reverse bias voltage. In this case, the THz time-domain signals are detected by use of a lock-

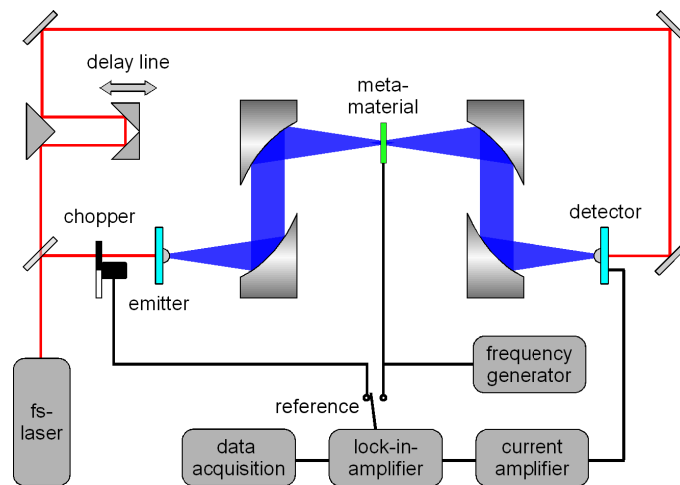


Fig. 3. Time-domain setup for the THz transmission measurements through the metamaterial device with externally tunable bias supply. For the experiments performed under DC voltage on the metamaterial we used a mechanical chopper wheel as reference source for the lock-in amplifier. For the measurements with modulated bias voltage, the modulation signal was used as reference signal.

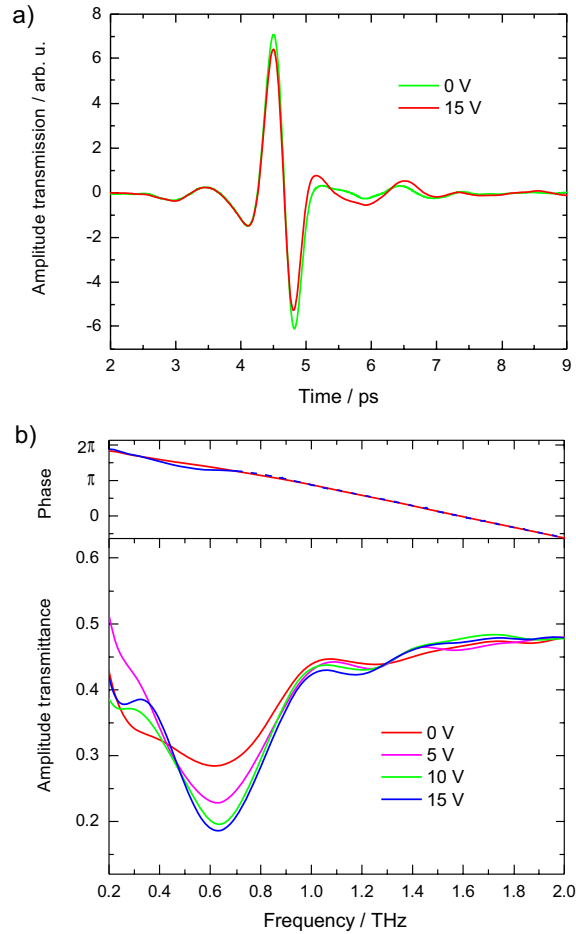


Fig. 4. Amplitude transmission of the metamaterial device for different voltages a) in the time-domain b) in the frequency-domain in magnitude and phase.

in amplifier and a mechanical chopper and then Fourier-transformed into the frequency-domain. The obtained transmission spectra are normalized by a reference spectrum without sample to obtain the amplitude transmittance of the device. We finally applied a Fourier filtering algorithm to remove spurious oscillations from the spectrum caused by multiple reflections within the GaAs substrate. This filtering process, however, reduces the frequency resolution to 70 GHz.

In Fig. 4, the amplitude transmittance of the THz device is plotted in both the time- and the frequency-domain for different values of the applied reverse bias voltage. As expected from our preliminary considerations, increasing the reverse bias voltage leads to the formation of a stop band in the vicinity of the resonance frequency at about 0.63 THz, where a marginal blue shift is observed. For voltages above 10 V the modulation depth starts to saturate. Note, that the phase spectrum is only slightly affected by the applied bias voltage.

A well established quantity for the performance of a modulator is the achieved relative change in the amplitude transmittance T given by

$$M_{DC} = \frac{T(0V) - T(U_{max})}{T(0V)}$$

where U_{max} is the maximum applied voltage. As shown in Fig. 4(b) increasing the magnitude of the reverse bias from 0 V to 15 V reduces the amplitude transmittance at the resonance frequency of 0.63 THz from $T(0\text{ V}) = 0.28$ to $T(15\text{ V}) = 0.18$, leading to $M_{DC} = 36\%$. In terms of intensity this corresponds to a value of $M_{DC}^{int} = (0.28^2 - 0.18^2)/0.28^2 = 59\%$. This is quite high in comparison with other electrically tunable metamaterial approaches [14, 15].

3.3. High frequency THz modulation

By applying a modulated bias voltage instead of a DC voltage to the structure, the THz beam transmitted through the metamaterial can be actively amplitude modulated. For a quantitative characterization of this modulation we removed the mechanical chopper from the THz detection setup and employed the metamaterial device itself as an electrical chopper. This is achieved by applying a modulated bias voltage to the metamaterial as well as to the lock-in amplifier as reference signal (see Fig. 3). With this configuration, the voltage output of the lock-in amplifier is proportional to the difference between the maximum and the minimum of the modulated THz field. By this method, we can directly measure the magnitude of the THz field modulation for different modulation frequencies. For the following experiments we used a square wave modulated bias voltage alternating between -13.3 V and 0 V.

To verify the accuracy of the proposed technique we exemplarily compared the resulting THz

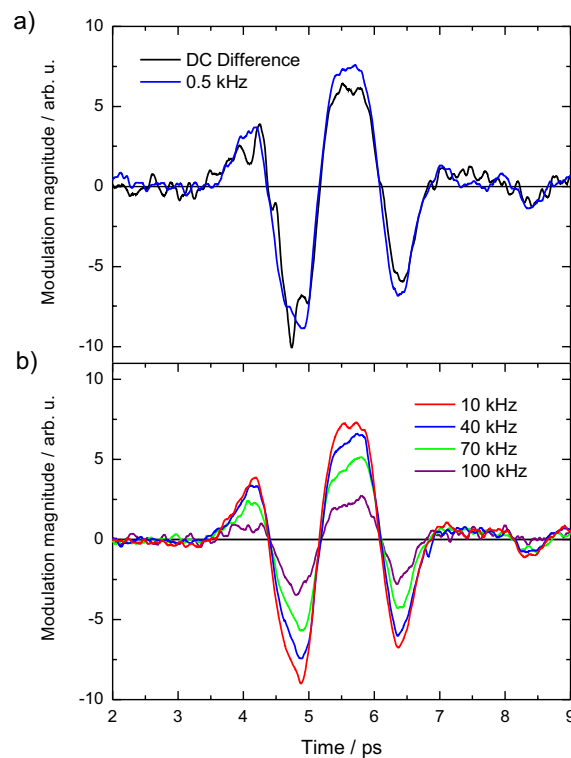


Fig. 5. a) Comparison of the directly measured THz time-domain difference signal of the modulated THz field at a modulation frequency of 0.5 kHz with the difference calculated from separately measured THz signals at the corresponding DC voltages. Both techniques deliver equivalent results for the modulation magnitude of the metamaterial-based THz modulator. b) THz time-domain difference signal for various modulation frequencies.

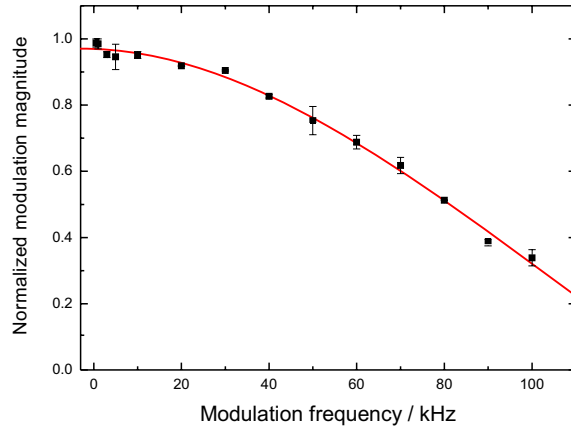


Fig. 6. Normalized modulation magnitude of the THz field in dependence of the modulation frequency.

time-domain difference signal at a modulation frequency of 0.5 kHz with the difference calculated from separately measured THz signals at the DC voltages of -13.3 V and 0 V, respectively. In the latter case, the time-domain signals were conventionally measured with the mechanical chopper inserted in the detection system. As shown in Fig. 5(a) the two difference signals obtained by the different techniques are in good agreement and confirm that the presented method is reliable for the determination of the modulation magnitude.

To analyze the modulation speed of the metamaterial-based modulator we followed this approach to measure the modulation magnitude for various modulation frequencies up to 100 kHz, which is the detection limit of the used lock-in amplifier. An exemplary excerpt of the recorded curves is presented in Fig. 5(b). As expected from the discussion in section 3.1, the magnitude of the modulation decreases for increasing modulation frequencies. This decrease is quite uniformly and well-described by a multiplicative, time-independent factor.

To quantify the frequency response of the device, we determined the peak-to-peak value of the recorded difference signals at each measured modulation frequency and normalized these values by their maximum. The result is presented in Fig. 6. As can be seen, the 50% cutoff frequency of the relative modulation depth is located at 80 kHz. This is in good agreement with the value estimated from the electric circuit measurements described in section 3.1. The attained modulation speed is about one order of magnitude higher in comparison with a conventional semiconductor THz modulator [20] and is comparable with the modulation speed measurement of the first reported electrically tunable THz metamaterial [14, 16], which in contrast to our design is polarization sensitive.

The results presented here refer to broadband THz pulses. However, by combining these results with the DC transmission spectrum shown in Fig. 4(b), we can approximate the relative modulation magnitude even for a monochromatic THz wave, which is given by

$$M(f, \nu) = \frac{T_{max} - T_{min}}{T_{max}}$$

where f is the modulation frequency, ν the frequency of the THz wave and T the amplitude transmittance. Since the pulse length of the THz pulses in our experiments is much smaller than the time constant of the charging and discharging process of the depletion zone, every pulse probes a quasi steady-state of the metamaterial. Therefore, the spectrum of the pulses passing

the uncharged device is equal to the DC transmission spectrum at 0 V, and the spectrum of the pulses probing the maximum loaded device is equal to the DC transmission spectrum at the peak value of the applied voltage signal. Hence, the maximum and the minimum transmittance of a modulated monochromatic THz wave is given by the corresponding DC transmission spectra. However, the decrease of the modulation magnitude for increasing modulation frequencies must be taken into account. As shown in this section, this dependence can be described by a multiplicative factor $\chi(f)$, which is represented in Fig. 6. The relative modulation magnitude of a monochromatic THz wave can therefore be estimated as

$$M(f, v) = \chi(f)M_{DC}(v)$$

where $M_{DC}(v)$ is the relative change in the DC transmission spectrum (as shown in Fig. 4(b)) at the peak values of the applied voltage signal. To give an example: the relative modulation magnitude of a monochromatic THz wave at 0.63 THz modulated by a 80 kHz bias signal with an amplitude of 15 V is approximately $M(80\text{kHz}, 0.63\text{THz}) \approx 0.5 \cdot 36\% = 18\%$

4. Conclusion

In conclusion, we have presented an electrically tunable metamaterial-based wave modulator operating in the THz frequency range. The implemented structure consists of an array of gold crosses fabricated on top of an n-doped GaAs layer, where the in-plane four-fold rotational symmetry of the used cross structure leads to a polarization-independent behavior. The structure exhibits a maximum amplitude modulation depth of 36% at the resonance frequency of 0.63 THz. We further demonstrated the fast modulation of a THz wave for modulation frequencies up to 100 kHz. Due to the simple structure design the layout can be easily scaled down in order to shift the operating range to higher frequencies. The structure thus offers a wide variety of applications from high-sensitive spectroscopy to short-range secure THz communication.

So far, the presented metamaterial structure has not been optimized with respect to the maximum achievable modulation depth, modulation speed and absolute transmission. For example, local doping techniques instead of a homogeneously doped top layer would provide further improvements. Since only the area between the ends of the crosses is crucial for the tunability of the metamaterial, the restriction of the n-doping to these regions would highly enhance the overall THz transmission and thus increase the maximum modulation depth. Furthermore, if only the area between the crossbars in one direction is doped, the proposed metamaterial enables the electric control of the polarization state of the transmitted THz wave.

Acknowledgment

The authors would like to acknowledge support from the Special Graduate Studies Program Graduiertenkolleg-792 "Nonlinear Optics and Ultrafast Physics" of the German Science Foundation (DFG).